Laboratori Nazionali di Frascati

LNF-63/7 (1963)

N. Cabibbo, G. Da Prato, G. De Franceschi, U. Mosco: ABSORPTION OF $\gamma$-RAYS IN CRYSTALS AND THE PRODUCTION AND ANALYSIS OF LINEARLY POLARIZED $\gamma$-RAYS.

Estratto da: Nuovo Cimento, 27, 979 (1963).

IL NUOVO CIMENTO VOL. XXVII, N. 4 16 Febbraio 1963

# Absorption of $\gamma$-Rays in Crystals and the Production and Analysis of Linearly Polarized $\gamma$-Rays.

N. CABIBBO

*Laboratori Nazionali di Frascati del CNEN - Roma*
*Istituto di Fisica dell'Università - Roma*

G. DA PRATO, G. DE FRANCESCHI and U. MOSCO

*Laboratori Nazionali di Frascati del CNEN - Roma*

(ricevuto il 29 Settembre 1962)

**Summary.** — We study the coherence effects on the total pair production cross-section in crystals at high energy. These effects are dependent on the photon polarization, and can be used for the production and the analysis of linearly polarized $\gamma$-ray beams.

## 1. – Introduction.

The possibility of coherence effects in electrodynamic processes (bremsstrahlung and pair production) on crystals at high-energy has been known for a long time (1); extensive theoretical work in this subject is due to ÜBERALL (2). The predicted effects were found (3,4) and there is now an excellent

(1) E. S. WILLIAMS: *Kgl. Dan. Viden., Sel., Mat. Fys. Medd.*, **13**, 4 (1935); B. FERRETTI: *Nuovo Cimento*, **7**, 118 (1950); M. L. TER-MIKAELYAN: *Žurn. Èksp. Teor. Fiz.*, **25**, 296 (1953); F. J. DYSON and H. ÜBERALL: *Phys. Rev.*, **99**, 604 (1955).

(2) H. ÜBERALL: *Phys. Rev.*, **103**, 1055 (1956); **107**, 223 (1957); L. I. SCHIFF: *Phys. Rev.*, **117**, 1394 (1960).

(3) W. K. H. PANOFSKY and A. N. S. SAXENA: *Phys. Rev. Lett.*, **2**, 219 (1959); O. R. FRISCH and D. H. OLSON: *Phys. Rev. Lett.*, **3**, 141 (1959).

(4) G. BOLOGNA, G. DIAMBRINI and G. P. MURTAS: *Phys. Rev. Lett.*, **4**, 134 (1960); G. BARBIELLINI, G. BOLOGNA, G. DIAMBRINI and G. P. MURTAS: *Phys. Rev. Lett.*, **8**, 112 (1962); *Phys. Rev. Lett.*, **8**, 454 (1962); *Phys. Rev. Lett.*, **9**, 46 (1962) (erratum).

agreement between theory and experiment. In this paper we report some work done by us on the interference effects observable in the total cross-section for pair production on crystals, and its dependence on the polarization of the incoming $\gamma$-rays.

At high energy the total cross-section for pair production is essentially equal to the cross-section for photon absorption; the fact that this cross-section is found in a crystal to depend on the photon linear polarization opens new possibilities for the production and analysis of linearly polarized $\gamma$-rays [5].

The dependence on the polarization of the absorption cross-section can be at most of the form [6],

$$\Sigma(\boldsymbol{\epsilon}) = A + B(\boldsymbol{\epsilon}\cdot\boldsymbol{t})^2 , \tag{1}$$

where $\boldsymbol{t}$ is a unit vector in a direction orthogonal to the momentum of the photons and $\boldsymbol{\epsilon}$ the polarization vector. In a crystal the direction $\boldsymbol{t}$ is related to the orientation of the lattice.

Photons which are polarized along $\boldsymbol{t}$ are absorbed with a mean free path $(A+B)^{-1}$, while those polarized orthogonal to $\boldsymbol{t}$ have a mean free path $A^{-1}$.

In passing through a thick crystal the two polarization components will suffer different attenuation and the surviving beam will be partially linearly polarized. The polarization will increase with the length traversed, and tend to 1 for infinite thickness (the intensity will in the meantime tend to zero).

Let's call $\Sigma^{\perp}$ and $\Sigma^{\parallel}$ the cross-sections for the two polarization states and introduce a parameter $E$:

$$E = \frac{\Sigma^{\perp} - \Sigma^{\parallel}}{\Sigma^{\perp} + \Sigma^{\parallel}} . \tag{2}$$

If the beam (originally unpolarized) passes through a crystal of thickness $x$ the resulting polarization will be [5]

$$P(x) = \operatorname{tgh}\left[\tfrac{1}{2}x(\Sigma^{\perp} - \Sigma^{\parallel})\right] . \tag{3}$$

The attenuation of the beam intensity will be

$$I(x)/I(0) = \exp\left[-E^{-1}\operatorname{tgh}^{-1}P(x)\right](1 - P^2(x))^{-\frac{1}{2}} . \tag{4}$$

[5] N. CABIBBO, G. DA PRATO, G. DE FRANCESCHI and U. MOSCO: *Phys. Rev. Lett.*, 6, 270 (1962).

[6] We consider cross-sections per unit volume (equal to the cross-section per nucleus multiplied by the number of nuclei per unit volume). These cross-sections can be directly interpreted as inverse of the mean free path.

If the beam had a linear polarization $\boldsymbol{Q}$, making an angle $\varphi$ with $\boldsymbol{t}$, the attenuation will depend on $\varphi$

$$[I(x)/I(0)]_{\boldsymbol{Q}} = [I(x)/I(0)]_{\boldsymbol{Q}=0}(1 + |\boldsymbol{Q}|P(x)\cos 2\varphi) \,. \tag{5}$$

It is therefore possible to derive $\boldsymbol{Q}$ from a measurement of the attenuation at different values of $\varphi$.

The effectiveness of a crystal as a polarizer depends on the value obtainable for $P(x)$ with acceptable intensity losses and reasonable physical dimensions of the crystal.

This can be judged from the value of $E$ as shown in Fig. 1 in which we plot $I(x)/I(0)$ as a function of $P(x)$ for different values of $E$ (eq. (4)).

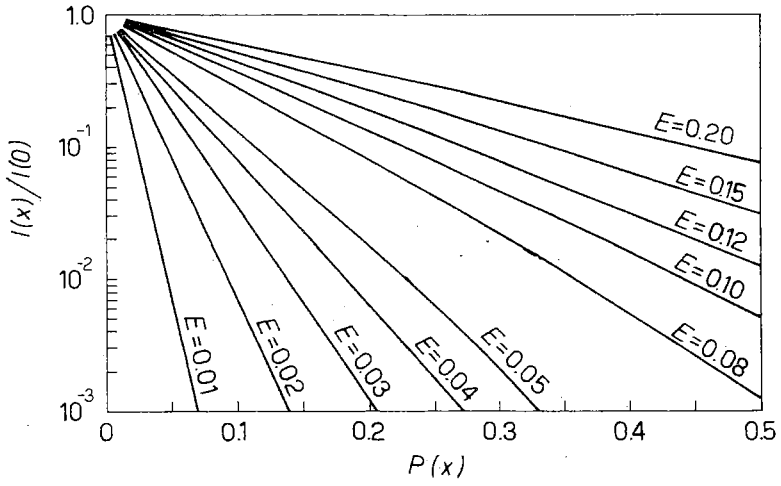


Fig. 1. – Relation between the attenuation of an unpolarized beam and the obtained polarization for different values of $E$.

If one puts a limit on the acceptable intensity loss: $I(x)/I(0) \geqslant 0.01$, a reasonable polarization $P \sim 20\,\%$ can be obtained if $E \sim 0.05$ or greater.

In the use as an analyser smaller values of $P$ (say $P \sim 5\,\%$) are already useful, and can be realized for $E \sim 0.01$.

It is possible to cross calibrate pairs of equal crystals using the first as a polarizer, the second as an analyser. This is a unique feature in this energy range and allows a direct measurement of the polarizing power $P(x)$.

In the following sections we give the details of the computations and the numerical results obtained in the case of crystals of silicon (at room temperature) and copper (at liquid nitrogen temperature, 77 °K). Both these crystals can probably be obtained in large sizes. It is found that the values of $E$ increase with the photon energy, $\omega$, and are larger for Cu than for Si.

Our results show that these crystals can be used as analysers ($E \sim 0.01$) for $\omega \geqslant 1$ GeV and as polarizers ($E = 0.05$) for $\omega \geqslant 6$ GeV.

In Section 2 we give the general formulas for the evaluation of total pair production in crystals.

In Section 3 we give the numerical results obtained for the said crystals and discuss them.

## 2. – General treatment.

In this section we evaluate the total cross-section for pair production on a crystal in the first Born approximation.

The techniques used are essentially those given in the papers by ÜBERALL [2] in which more details and justifications can be found.

We consider a cubic lattice, where $a$ is the lattice constant, in a reference system where the three axes, $x$, $y$, $z$ coincide with the main axes of the crystal.

The differential cross-section for pair production on an external electrostatic field is, in the first Born approximation, proportional to the square of the Fourier transform of the potential:

$$V(\boldsymbol{q}) = (2\pi)^{-\frac{3}{2}} \int V(x) \exp[i\boldsymbol{q}\boldsymbol{x}] \mathrm{d}^3x \,, \tag{6}$$

where $\boldsymbol{q}$ is the momentum transfer to the target. If we neglect for the moment the thermal and zero point motion of the nuclei, the crystal is a periodic structure, so that the Fourier transform $V(\boldsymbol{q})$ is different from zero only if the momentum transfer $\boldsymbol{q}$ coincides with one of the points of the reciprocal lattice.

One can write:

$$[V(\boldsymbol{q})]^2 = [V_0(\boldsymbol{q})]^2 \frac{(2\pi)^3}{a^3} N \sum_{\boldsymbol{g}} D(\boldsymbol{g}) \delta(\boldsymbol{q} - \boldsymbol{g}) \,. \tag{7}$$

The sum is over the points of the reciprocal lattice, $\boldsymbol{g}$. $V_0(\boldsymbol{g})$ is the Fourier transform of the Coulomb potential of a single nucleus, $D(\boldsymbol{g})$ gives the «strength» of the point $\boldsymbol{g}$.

Note that $[V(\boldsymbol{g})]^2$ is proportional to the number of atoms in the crystal.

To get cross sections per unit volume [6] it will be sufficient to take $N$ equal to the number of atoms per unit volume.

If the real lattice is simple cubic, the reciprocal lattice is also simple cubic with lattice constant equal to $2\pi/a$, with $D(\boldsymbol{g}) = 1$. Each point of the reciprocal lattice is denoted by three entire numbers:

$$\boldsymbol{g} \equiv (l, m, n) \,.$$

The reciprocal lattice for more complex cubic structures like the face centered (FCC) or the diamond lattice, can also be considered as simple cubic, the only difference being in $D(\boldsymbol{g})$, which is derived for these lattices in Appendix II.

Using (7) we find the total cross-section (per unit volume) for pair production on a crystal by a photon of momentum $\boldsymbol{k}$ and polarization $\boldsymbol{\epsilon}$ given by

$$\sum(\boldsymbol{k}, \boldsymbol{\epsilon}) = \frac{(2\pi)^3}{a^3} N \sum_{\boldsymbol{g}}^{*} D(\boldsymbol{g}) \left[\frac{\partial\sigma^0(\boldsymbol{k}, \boldsymbol{\epsilon}, \boldsymbol{q})}{\partial^3\boldsymbol{q}}\right]_{\boldsymbol{q}=\boldsymbol{g}} . \tag{8}$$

where $\partial\sigma^0/\partial^3\boldsymbol{q}$ is the cross-section for pair production on a single nucleus, differential in respect to the momentum transfer $\boldsymbol{q}$.

The asterisk on the summation symbol reminds that this summation is extended only over those points in the reciprocal lattice which correspond to kinematically possible values of the momentum transfer.

This simple treatment is incomplete because we have neglected the thermal and zero point motions of the nuclei due to which the crystal is not a true periodical static structure. As shown by ÜBERALL this fact can be taken into account with good approximation by introducing in (8) a factor $\exp[-Aq^2]$, where $A$ is connected with the mean square value of the distance of the nuclei from their equilibrium positions, and adding an incoherent contribution obtained by integrating the differential Bethe-Heitler cross-section with a factor $(1-\exp[-Aq^2])$. We write therefore

$$\Sigma(\boldsymbol{k}, \boldsymbol{\epsilon}) = \Sigma_I(\boldsymbol{k}, \boldsymbol{\epsilon}) + \Sigma_T(\boldsymbol{k}) , \tag{9}$$

where

$$\Sigma_I(\boldsymbol{k}, \boldsymbol{\epsilon}) = \frac{(2\pi)^3}{a^3} N \sum_{\boldsymbol{g}}^{*} D(\boldsymbol{g}) \exp[-Aq^2] \left[\frac{\partial\sigma^0(\boldsymbol{k}, \boldsymbol{\epsilon}, \boldsymbol{q})}{\partial^3\boldsymbol{q}}\right]_{\boldsymbol{q}=\boldsymbol{g}} , \tag{10}$$

$$\Sigma_T(\boldsymbol{k}) = N\int \mathrm{d}^3\boldsymbol{q}(1-\exp[-Aq^2]) \frac{\partial\sigma^0(\boldsymbol{k}, \boldsymbol{\epsilon}, \boldsymbol{q})}{\partial^3\boldsymbol{q}} . \tag{11}$$

Note that $\Sigma_T$ does not depend on $\boldsymbol{\epsilon}$, since the right-hand side can depend only on $\boldsymbol{k}$ and $\boldsymbol{\epsilon}$, and $\boldsymbol{k}\boldsymbol{\epsilon} = 0$.

We can therefore substitute the differential cross-section for unpolarized photons under the integral:

$$\Sigma_T(\mathrm{ff}\boldsymbol{k}) = N\int \mathrm{d}^3\boldsymbol{q}(1-\exp[-Aq^2]) \frac{\partial\sigma^0(\boldsymbol{k}, \boldsymbol{q})}{\partial^3\boldsymbol{q}} . \tag{11'}$$

Let us consider eq. (10): the kinematically allowed values of $\boldsymbol{q}$ are contained in a sphere with center in $\boldsymbol{q} = \boldsymbol{k}$ and radius equal to $\sqrt{|\boldsymbol{k}|^2 - 4m_e^2}$.

The minimum allowed value is:

$$\delta = |\boldsymbol{k}| - \sqrt{|\boldsymbol{k}|^2 - 4m_e^2} \simeq \frac{2m_e^2}{\omega}, \tag{12}$$

where $\omega = |\boldsymbol{k}|$ is the photon energy.

The differential cross-section (for unpolarized photons) $\partial^3\sigma^0(\boldsymbol{k}, \boldsymbol{q})/\partial^3\boldsymbol{q}$ decreases [7] rapidly when $q^{\parallel}$, the component of $\boldsymbol{q}$ along $\boldsymbol{k}$, increases; the main contributions to the sum come from the region $\delta < q^{\parallel} \leqslant 4\delta$.

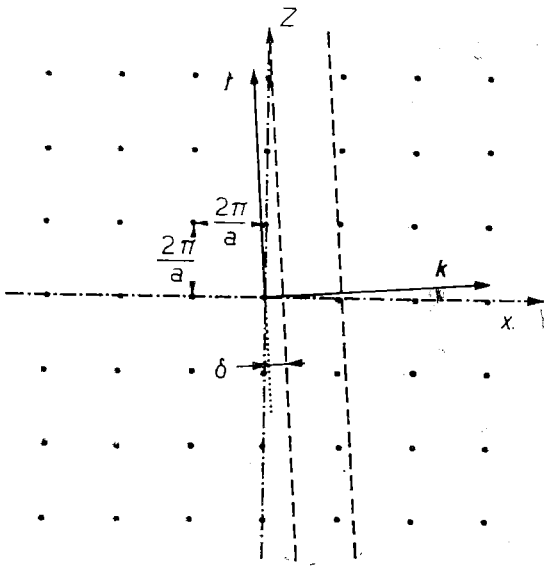


Fig. 2. – Position of the allowed region of $\boldsymbol{q}$ in the reciprocal lattice for $\alpha \approx 0$ (Si, $\omega = 1$ GeV).

The main limitation on the values of the component of $\boldsymbol{q}$ orthogonal to $\boldsymbol{k}$ comes from the exponential factor $\exp[-Aq^2]$; since for all the crystals we consider $A \sim 200\, m_e^{-2}$, this factor cuts off values of $q \geqslant 0.1\, m_e$.

In this way the relevant values of $\boldsymbol{q}$ are restricted to a disk-shaped region (pancake) displaced by $\delta$ from the origin, orthogonal to $\boldsymbol{k}$, of thickness $\sim 3\delta$ and radius $\sim 0.1\, m_e$.

Suppose that the $\gamma$-rays hit the crystal in such a way that $\boldsymbol{k}$ lies in the (010) plane, making a small angle $\alpha$ with the (100) axis; Fig. 2 gives an idea of the position of the pancake in respect to the reciprocal lattice points [8]. The scale is appropriate for a crystal of silicon at $\omega = 1$ GeV.

When we increase $\alpha$ new rows of the reciprocal lattice are included in the pancake and the interference contribution is modified.

Already at this energy the main contribution comes from the first lattice plane ($q_x = 0$, $l = 0$).

According to eq. (1) a polar plot of the cross section $\Sigma(\boldsymbol{k}, \boldsymbol{\epsilon})$ on the plane orthogonal to $\boldsymbol{k}$ is an ellipse where, depending on the sign of $B$, $\boldsymbol{t}$ is in the direction of the minor or the major axis.

Since the (010) plane ($q_y = 0$, $m = 0$) is a symmetry plane in the situation of Fig. 2, one of the axes of the ellipse must be in this plane, and we can select $\boldsymbol{t}$ to coincide with its direction.

[7] R. JOST, J. M. LUTTINGER and M. SLOTNICK: *Phys. Rev.*, **80**, 189 (1950).

[8] Each point in this figure represents a row of points in the reciprocal lattice.

In order to evaluate the polarizing power (eqs. (2) to (5)) we need the difference of the cross-sections for $\boldsymbol{\epsilon} = \boldsymbol{y}$ (unit vector along the $y$ axis, orthogonal to $\boldsymbol{t}$) and $\boldsymbol{\epsilon} = \boldsymbol{t}$, and their average.

The latter is obtained by introducing the average differential cross-section in eqs. (9) and (10):

$$\frac{1}{2}(\Sigma^{\perp} + \Sigma^{\parallel}) = \Sigma_I(\boldsymbol{k}) + \Sigma_T(\boldsymbol{k}) , \tag{13}$$

where $\Sigma_T(\boldsymbol{k})$ is given in eq. (11′) and

$$\Sigma_I(\boldsymbol{k}) = \frac{(2\pi)^3}{a^3} N \sum_{\boldsymbol{g}}^{*} D(\boldsymbol{g}) \exp\left[-A\,|\boldsymbol{g}|^2\right] \frac{\partial\sigma^0(\boldsymbol{k}, \boldsymbol{g})}{\partial^3\boldsymbol{g}} ; \tag{14}$$

the difference is

$$\Sigma^{\perp} - \Sigma^{\parallel} = \frac{(2\pi)^3}{a^3} N \sum_{\boldsymbol{g}}^{*} D(\boldsymbol{g}) \exp\left[-A\,|\boldsymbol{g}|^2\right] \left[\frac{\partial\sigma^0(\boldsymbol{k}, \boldsymbol{y}, \boldsymbol{g})}{\partial^3\boldsymbol{g}} - \frac{\partial\sigma^0(\boldsymbol{k}, \boldsymbol{t}, \boldsymbol{g})}{\partial^3\boldsymbol{g}}\right] . \tag{15}$$

The dependence of $\partial\sigma^0(\boldsymbol{k}, \boldsymbol{\epsilon}, \boldsymbol{q})/\partial^3\boldsymbol{q}$ on $\boldsymbol{\epsilon}$ can be of the form (since $(\boldsymbol{k}\cdot\boldsymbol{\epsilon}) = 0$)

$$\frac{\partial\sigma^0}{\partial^3\boldsymbol{q}} = L + M(\boldsymbol{\epsilon}\cdot\boldsymbol{q})^2 , \tag{16}$$

where $L$ and $M$ are scalar functions of $\boldsymbol{k}$, $\boldsymbol{q}$.

$$\frac{\partial\sigma^0(\boldsymbol{k}, \boldsymbol{y}, \boldsymbol{g})}{\partial^3\boldsymbol{g}} - \frac{\partial\sigma^0(\boldsymbol{k}, \boldsymbol{t}, \boldsymbol{g})}{\partial^3\boldsymbol{g}} = M(\boldsymbol{k}, \boldsymbol{g})[(\boldsymbol{y}\cdot\boldsymbol{g})^2 - (\boldsymbol{t}\cdot\boldsymbol{g})^2] = \\ = -M(\boldsymbol{k}, \boldsymbol{g})\,|\boldsymbol{g}^{\perp}|^2 \cos 2\theta , \tag{17}$$

where $|\boldsymbol{g}^{\perp}|$ is the component of $\boldsymbol{g}$ orthogonal to $\boldsymbol{k}$ and $\theta$ is the angle between $\boldsymbol{g}$ and $\boldsymbol{t}$. We can therefore write:

$$\Sigma^{\perp} - \Sigma^{\parallel} = -\frac{(2\pi)^3}{a^3} N \sum_{\boldsymbol{g}}^{*} D(\boldsymbol{g}) \exp\left[-A\,|\boldsymbol{g}|^2\right] M(\boldsymbol{k}, \boldsymbol{g})\,|\boldsymbol{g}^{\perp}|^2 \cos 2\theta . \tag{15′}$$

The formulas for $\partial\sigma^0/\partial^3\boldsymbol{g}$ and $M(\boldsymbol{k}, \boldsymbol{g})$ are given in the Appendix I (eqs. (A.1) and (A.2)).

The polarizing effect of the crystal can now be understood in the following way: when $\alpha$ is small, the points $\boldsymbol{g}$ of the reciprocal lattice which contribute to the sum in eq. (15′) are clustered around the $z$-axis, so that the dependence of $\partial\sigma^0/\partial^3\boldsymbol{q}$ on $\boldsymbol{\epsilon}$ causes a finite value of $\Sigma^{\perp} - \Sigma^{\parallel}$.

For FCC and diamond lattices better results are obtained when the $\boldsymbol{k}$ is nearly orthogonal to the (101) plane as shown in Fig. 3 because this plane has an higher concentration of points with $D(\boldsymbol{g}) \neq 0$.

One can use the same equation given here, choosing $\alpha \sim \pi/4$.

### 3. – Results and discussion.

We have done numerical evaluations of the parameter $E$ at different energies and angles. We have studied in detail the energy regions around 1 GeV, relevant for the existing synchrotrons and linear accelerators, around 6 GeV, relevant for the new synchrotrons at Desy and CEA, and around 40 GeV which could be reached by the future Stanford linear accelerator.

The following choice of parameters was done:

TABLE I.

| | Cu (77 °K) | Si (300 °K) |
|---|---|---|
| $a$ | 935.4 $m_e^{-1}$ | 1400 $m_e^{-1}$ |
| $b$ | 1360 $m_e^{-2}$ | 2112 $m_e^{-2}$ |
| $A$ | 166 $m_e^{-2}$ | 282 $m_e^{-2}$ |

The screening form factor $F(q^2)$ was taken in the form

$$F(q^2) = \frac{1}{1 + bq^2}, \tag{17}$$

with $b$ given in Table I.

We have evaluated first the thermal contribution (eq. (11′)). Integration over the angles does not involve the exponential factor, and was evaluated by JOST *et al.* [7], the integral in eq. (11′) can be therefore reduced to the form:

$$\Sigma_T(k_0) = N \int_{\alpha-(\alpha^2-1)^{\frac{1}{2}}}^{\alpha+(\alpha^2-1)^{\frac{1}{2}}} (1 - \exp[-4m_e^2 A Q^2]) \cdot P(Q, k_0)\, \mathrm{d}Q\,. \tag{18}$$

The symbols are defined in [7], see formulas (37), (39). This integral was evaluated numerically for the two crystals and for different energies; the results, shown in Fig. 4, are of the same order of magnitude of the Bethe-Heitler cross-section.

We have then evaluated the interference contributions (eqs. (14) and (15))

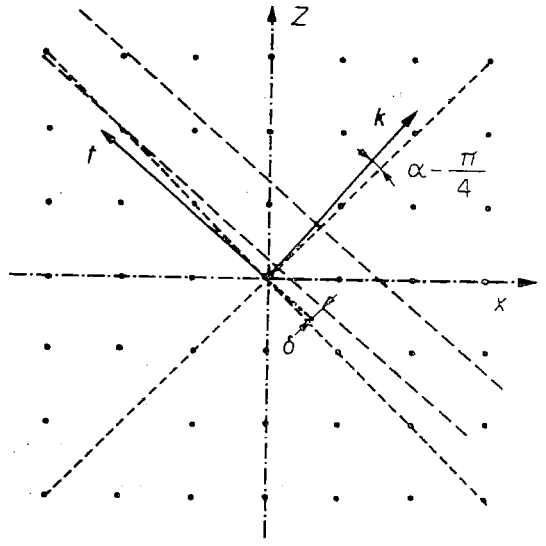


Fig. 3. – Same as Fig. 2, but with $\alpha \approx \pi/4$.

This was also done numerically. The sum was extended only over the points which give important contributions. The program for the electronic computer

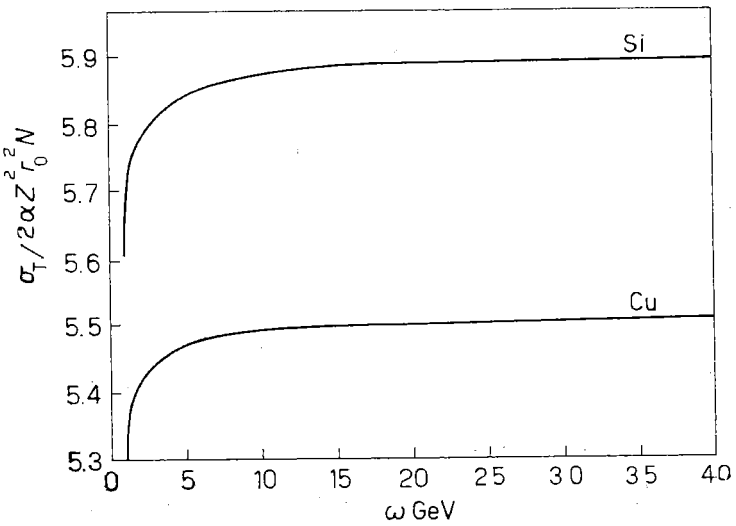


Fig. 4. – Incoherent contribution to the cross-section due to the thermal and zero-point motion of the nuclei.

had adjustable parameters wich fixed the number of planes in the reciprocal lattice (see Fig. 2), which were considered, the number of rows in each plane and the number of points in each row.

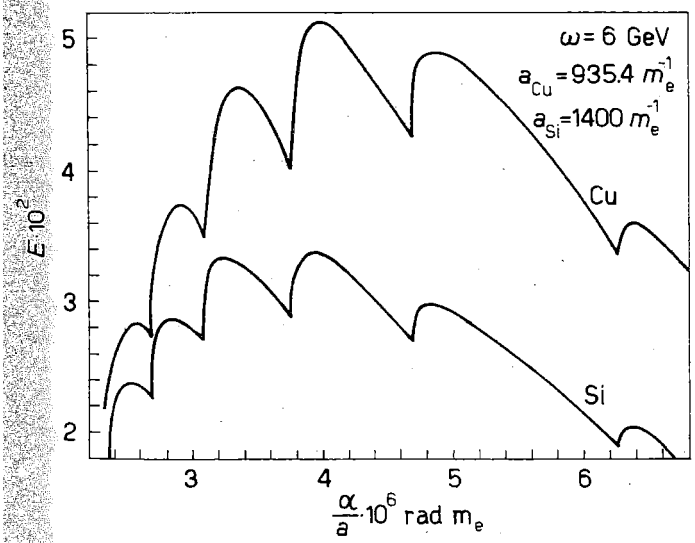


Fig. 5. – $E$ as a function of, $\alpha$, $\omega = 6$ GeV.

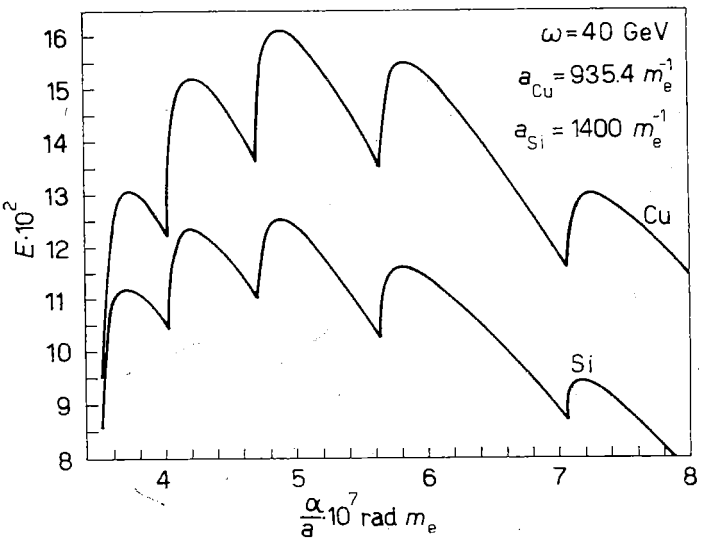


Fig. 6. – $E$ as a function of $\alpha$, $\omega = 40$ GeV.

At high energy ($\gtrsim 6$ GeV) the first plane ($l = 0$) was sufficient, while at 1 GeV the second plane ($l = 1$) gave a small but not negligible contribution. The number of rows and of points in each row were between 20 and 40.

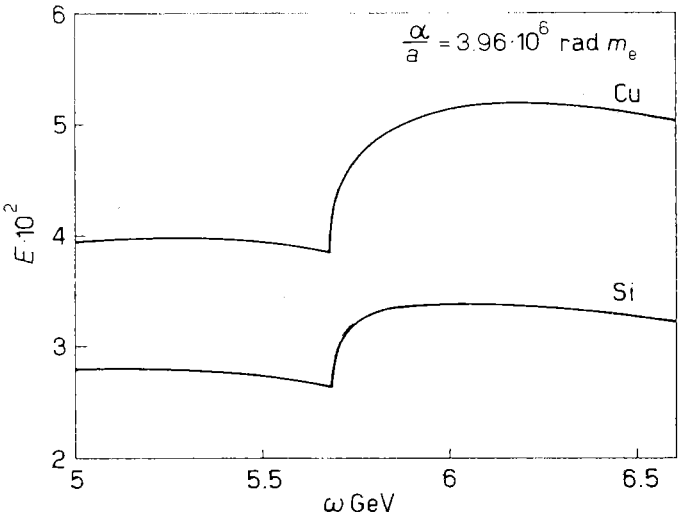


Fig. 7. – $E$ as a function of $\omega$, around $\omega = 6$ GeV, in Cu for $\alpha = 3.7$ mrad, in Si for $\alpha = 5.5$ mrad.

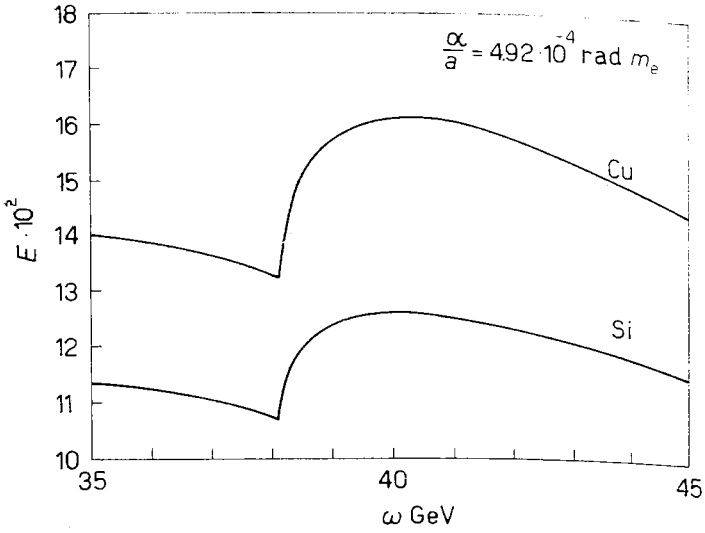


Fig. 8. – $E$ as a function of $\omega$, around $\omega = 40$ GeV, in Cu for $\alpha = 0.46$ mrad, in Si for $\alpha = 0.68$ mrad.

The same procedure was used for $\boldsymbol{k}$ near to the (101) axis ($\alpha \sim \pi/4$, see Fig. 3).

In the following we report only the data obtained in this situation, which gives larger values for $E$.

Figures 5, 6 give the values of $E$ as a function of $(\alpha - \pi/4)$ for energies $\omega = 6$ GeV, 40 GeV.

These figures are similar, and we note that:

1) The best value of $E$ increases with the energy, while the angle at which it occurs decreases.

Both these features are easily understood because the distance of the pancake from the origin decreases with the energy (eq. (12)).

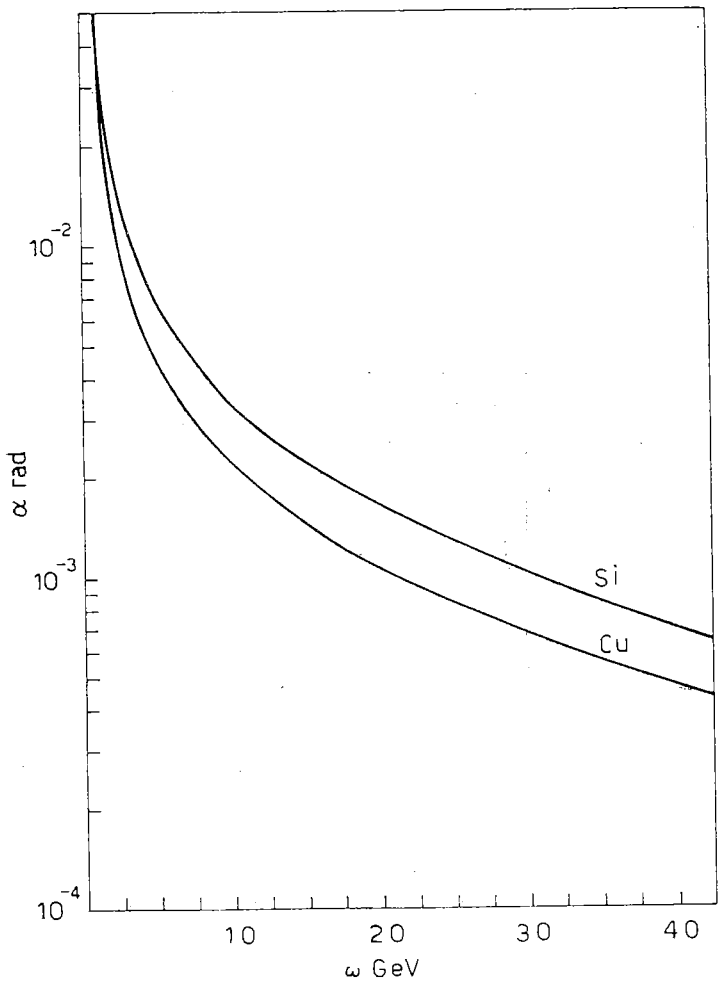


Fig. 9. – Variation of the optimum angle with the energy.

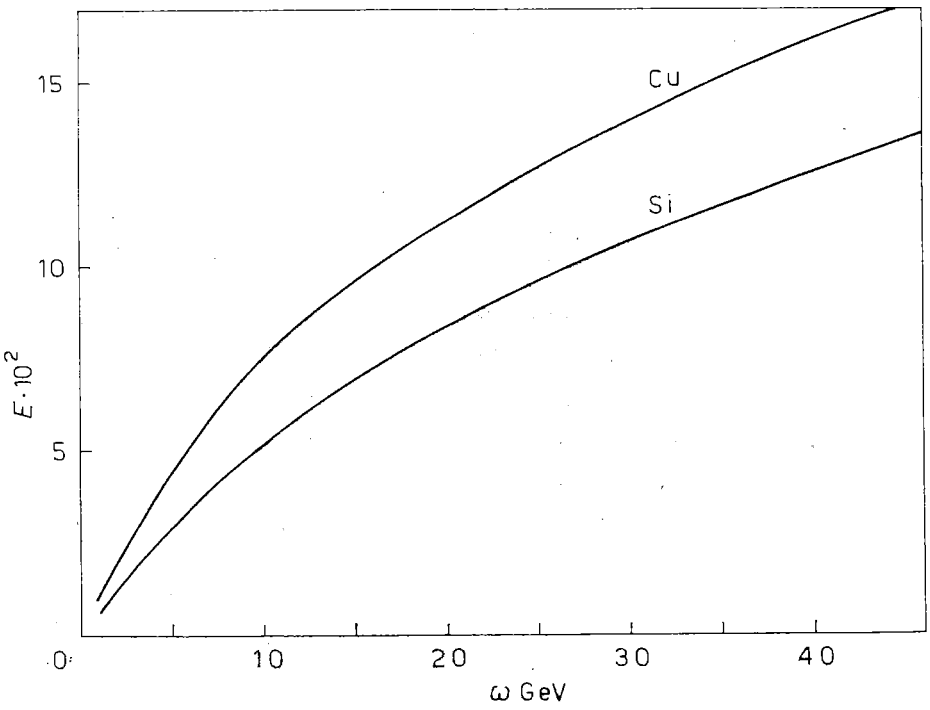


Fig. 10. – $E$ at the best angle as a function of the energy.

2) The function $E(\alpha, \omega)$ is not smooth; the discontinuities in its derivative are connected with the entrance in the allowed region of new rows of the first plane in the reciprocal lattice; a row with a certain value $n$ coincides

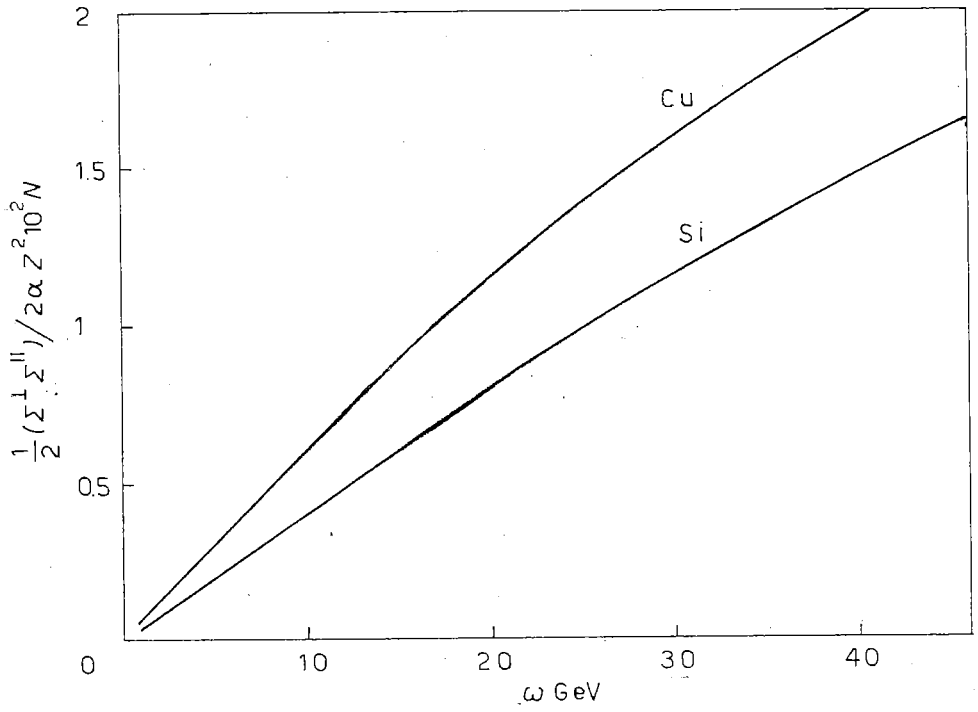


Fig. 11. – $\frac{1}{2}(\Sigma^{\perp} - \Sigma^{\parallel})$ at the best angle as a function of the energy.

with the surface of the allowed region when

$$\alpha - \frac{\pi}{4} = \frac{\delta a n}{\sqrt{2\pi}}, \tag{19}$$

the variable $\alpha/a$ used in the figures is such that the discontinuities appear at the same points, to emphasize the relation in eq. (19).

In the practical use of a crystal, one would have a given value of $\alpha$ but a photon beam with a continuous spectrum of energies.

In Fig. 7, 8, we give the dependence of $E$ on $\omega$ for the best values of $\alpha$ at $\omega = 6$ GeV and 40 GeV, obtained from the Fig. 5, 6.

This graphs are rather smooth, the discontinuities are also due to the disappearance of one of the rows in the first plane from the allowed region, and their positions can be obtained from eq. (19): Fig. 9, 10 and 11, give the best angle and the corresponding values of $E$ and of $\frac{1}{2}(\Sigma^{\perp} - \Sigma^{\parallel})$ as a function of $\omega$.

From the data presented here it is seen that the use of a crystal as a polarizer starts to be practical at some GeV, while its use as an analyser (where a smaller $P(x)$ is acceptable) can be already considered for photons of 1 GeV.

* * *

We are grateful to Prof. DIAMBRINI, and Drs. BARBIELLINI, BOLOGNA, MURTAS for interesting discussions of the interference effects in crystals, and to Dr. TURRIN and the members of the computer group of the Frascati Laboratories for their kind assistance in running the programs on the IBM 1620 computer.

## APPENDIX I

In this appendix we evaluate the differential cross-section $\partial\sigma^0(\boldsymbol{k}, \boldsymbol{\epsilon}, \boldsymbol{q})/\partial^3\boldsymbol{q}$ for pair production on nuclei which is needed in Section 2.

In the case of unpolarized photons this cross-section was obtained by JOST *et al.* [7] using a method based on the unitarity of the $S$-matrix; they obtain:

$$\begin{aligned}\frac{\partial^3\sigma^0(\boldsymbol{k}, \boldsymbol{q})}{\partial^3\boldsymbol{q}} = &- 2\alpha Z^2 r_0^2 m_e^2 \frac{1}{\pi\omega |\boldsymbol{q}|^4} \frac{1}{\beta^2}\Big\{-4|\boldsymbol{q}|^2(-2m_e^2 \ln\varrho + \tilde{v}(\beta - |\boldsymbol{q}|^2)) - \\ &- \frac{\beta^2 - 4|\boldsymbol{q}|^2\omega^2}{\beta^2}\Big[|\tilde{v}(\beta^2 - 4(|\boldsymbol{q}|^2 - \beta)(m_e^2 - 2|\boldsymbol{q}|^2)) - \\ &- \ln\varrho(\beta^2 + 2(\beta - |\boldsymbol{q}|^2)(2m_e^2 - |\boldsymbol{q}|^2) - 8m_e^2(|\boldsymbol{q}|^2 + m_e^2))\Big]\Big\},\end{aligned} \tag{A.1}$$

where:

$$\beta = 2(\boldsymbol{k}\cdot\boldsymbol{q})\,; \qquad \tilde{v} = \sqrt{1-\frac{4m_e^2}{\beta-|\boldsymbol{q}|^2}}\,; \qquad \varrho = \frac{1+\tilde{v}}{1-\tilde{v}}\,.$$

We also needed $M(\boldsymbol{k}, \boldsymbol{q})$ defined in eq. (16).

Let us select a particular $\boldsymbol{\epsilon}$, $\boldsymbol{\epsilon}^\perp$, orthogonal to the plane $(\boldsymbol{k}, \boldsymbol{q})$, and denote by $\boldsymbol{q}^\perp$ the component of $\boldsymbol{q}$ orthogonal to $\boldsymbol{k}$; one obtains:

$$M(\boldsymbol{k}, \boldsymbol{q})\,|\boldsymbol{q}^\perp|^2 = 2\left[\frac{\partial^3\sigma^0(\boldsymbol{k}, \boldsymbol{q})}{\partial^3\boldsymbol{q}} - \frac{\partial^3\sigma^0(\boldsymbol{k}, \boldsymbol{\epsilon}^\perp, \boldsymbol{q})}{\partial^3\boldsymbol{q}}\right]. \tag{A.2}$$

It is therefore necessary to evaluate the differential cross-section for $\boldsymbol{\epsilon} = \boldsymbol{\epsilon}^\perp$.

We prefer to do so by direct integration of the Bethe-Heitler formula ([9]):

$$\frac{\partial^3\sigma^0(\boldsymbol{k}, \boldsymbol{\epsilon}, \boldsymbol{q})}{\partial^3\boldsymbol{q}} = \frac{\alpha Z^2 r_0^2}{2\pi^2}\,\frac{(1-F(q^2))^2}{\omega q^4}\int\delta^4(k-p_+-p_--q)\,\frac{\mathrm{d}^3\boldsymbol{p}_+}{E_+}\,\frac{\mathrm{d}^3\boldsymbol{p}_-}{E_-}\,X\,, \tag{A.3}$$

where $(1-F)^2$ is the screening correction, $p_\pm = (\boldsymbol{p}_\pm, E_\pm)$ are the momenta of the produced electron and positron, and

$$X = 4\left[E_+\frac{(p_-\varepsilon)}{(p_-k)} + E_-\frac{(p_+\varepsilon)}{(p_+k)}\right]^2 - q^2\left[\frac{(p_-\varepsilon)}{(p_-k)} - \frac{(p_+\varepsilon)}{(p_+k)}\right]^2 + \\ + 2 + \frac{q^2\omega^2}{(p_-k)(p_+k)} + \frac{(p_+k)}{(p_-k)} + \frac{(p_-k)}{(p_+k)}\,. \tag{A.4}$$

The direct execution of the integral in the laboratory system is however cumbersome because of the complex angular relations between $\boldsymbol{k}$, $\boldsymbol{q}$, $\boldsymbol{p}_+$, $\boldsymbol{p}_-$.

It was found desirable to evaluate it in the rest frame of the produced electrons.

The integration is indeed Lorentz-invariant, but $X$ is not because of the appearance of quantities like $E_\pm$ and $\omega$.

This difficulty is met introducing a unit vector which is purely timelike in the lab. system:

$$n = (0, 0, 0, i) \quad \text{(in the lab. system)}\,, \tag{A.5}$$

so that in an invariant form:

$$\omega = -(kn)\,, \qquad E_\pm = -(p_\pm n)\,. \tag{A.6}$$

Another difficulty is that the first term in $X$, is not manifestly gauge-invariant (it is not equal to zero if we substitute $\boldsymbol{k}$ for $\boldsymbol{\epsilon}$).

---

([9]) J. M. JAUCH and F. ROHRLICH: *The Theory of Photons and Electrons* (Cambridge, Mass., 1955).

It can be however rendered gauge-invariant through rewriting it as

$$4\left|-(np_+)\frac{(p_-\varepsilon)}{(p_-k)}-(np_-)\frac{(p_+\varepsilon)}{(p_+k)}+(n\varepsilon)\right|^2, \tag{A.7}$$

if we substitute $\boldsymbol{k}$ for $\boldsymbol{\epsilon}$, we get:

$$4[-(np_+)-(np_-)+(nk)]^2=4(nq)^2=0\,, \tag{A.8}$$

since $q$ is purely spacelike in the lab. system.

With this modifications it is possible to evaluate the integral directly in the rest system of the two produced electrons. The computations are still lenghty but very straightforward.

We get:

$$\frac{\partial^3\sigma^0(\boldsymbol{k},\boldsymbol{\epsilon}^\perp,\boldsymbol{q})}{\partial^3\boldsymbol{q}}=-\frac{2\alpha Z^2r_0^2m_e^2}{\pi\omega q^4\beta^2}\left\{-4q^2\left(-2m_e^2\ln\varrho+\tilde{v}(\beta-q^2)\right)+-\frac{\beta^2-4q^2\omega^2}{\beta^2}\cdot\right. \tag{A.9}$$

$$\left.\cdot\left[\tilde{v}(q^2-\beta)(7q^2-\beta-2m_e^2)-\ln\varrho(\beta^2+2(\beta-q^2)(2m_e^2-q^2))-4m_e^2(q^2+m_e^2)\right]\right\},$$

from which, and eq. (2):

$$M(\boldsymbol{k},\boldsymbol{q})\,|\boldsymbol{q}^\perp|^2=\frac{2\alpha Z^2r_0^2}{\pi\beta^2\omega q^4}\,\frac{4q^2\omega^2-\beta^2}{\beta^2}\,\{\tilde{v}[2m_e^2(q^2-\beta)-q^4]-4m_e^2(q^2+m_e^2)\ln\varrho\}. \tag{A.10}$$

As a check we have obtained independently the result given by JOST *et al.* [7] eq. (A.1).

A physical check of these formulas is the following: when $\boldsymbol{v}$, the velocity of the electrons in the rest system, tends to zero, the pair will be produced in an $S$ state, and since the pair is produced by two photons (one is a virtual photon exchanged with the nucleus), in a state with charge conjugation $C=+1$, *i.e.* an $S'$ state, the pair will then behave as a single pseudoscalar particle. The matrix element for the photoproduction of such a particle on a Coulomb field is of the forms $\boldsymbol{\epsilon}\cdot\boldsymbol{k}\wedge\boldsymbol{q}$ so that in this limit ($\boldsymbol{v}=0$) the cross-section must vanish for $\boldsymbol{\epsilon}$ in the $\boldsymbol{k}$, $\boldsymbol{q}$, plane, and this requires

$$\lim_{v\to 0}\left[|\boldsymbol{q}^\perp|^2M(\boldsymbol{k},\boldsymbol{q})\right]\Big/\left[\frac{\partial^3\sigma(\boldsymbol{k},\boldsymbol{q})}{\partial^3\boldsymbol{q}}\right]=-2\,, \tag{A.11}$$

a relation satisfied by our eqs. (A.1) and (A.10).

## APPENDIX II

We evaluate here the strenght of the points of a reciprocal lattice for the cases in which the real lattice is face-centered cubic (FCC) and diamond.

We start from the fact that for a simple cubic crystal $D(\boldsymbol{g}) = 1$. The Coulomb potential in a crystal can be written as

$$V(\boldsymbol{x}) = \sum_{\xi_i} V^0(\boldsymbol{x} - \xi_i) , \tag{A.12}$$

where $V^0(\boldsymbol{x} - \xi_i)$ is the contribution of the $i$-th nucleus in position $\xi_i$. It follows:

$$V(\boldsymbol{g}) = V^0(\boldsymbol{g}) \sum_{\xi_i} \exp[i(\boldsymbol{g}\cdot\xi_i)] , \tag{A.13}$$

where $\boldsymbol{g}$ is one of the points of the reciprocal lattice (see eq. (6)).

A FCC lattice of lattice constant $a$ can be considered as a superposition of a simple cubic lattice plus three other simple cubic lattices obtained from the first by translations of $a/\sqrt{2}$ along the diagonals of the three faces of the basic cube.

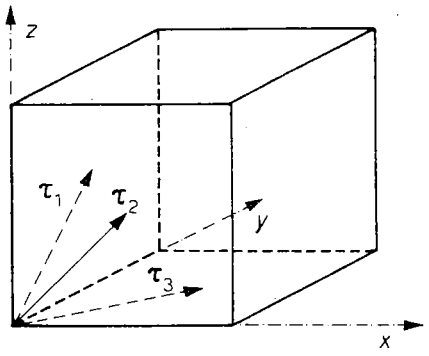


Fig. 12. – Basic cell of a FCC lattice.

In Fig. 12 we show the basic cubic cell with the three translation vectors.

We can therefore write

$$\sum_{\xi_i} \exp[i(\boldsymbol{g}\cdot\xi_i)] = \tag{A.14}$$

$$= \sum_{\xi_i}^{0} \exp[i(\boldsymbol{g}\cdot\xi_i)](1 + \exp[i(\boldsymbol{g}\cdot\tau_1)] + \exp[i(\boldsymbol{g}\cdot\tau_2)] + \exp[i(\boldsymbol{g}\cdot\tau_3)]) .$$

Where the sum is extended over the points at the vertices of the basic simple cubic lattice.

If we square this and remember that for a simple cubic lattice $D(\boldsymbol{g}) = 1$ we obtain (FCC lattice)

$$D(\boldsymbol{g}) = \tfrac{1}{4}(1 + \exp[i(\boldsymbol{g}\cdot\tau_1)] + \exp[i(\boldsymbol{g}\cdot\tau_2)] + \exp[i(\boldsymbol{g}\cdot\tau_3)])^2 . \tag{A.15}$$

If we remember that

$$\boldsymbol{g} \equiv \left(\frac{2\pi l}{a}, \frac{2\pi m}{a}, \frac{2\pi n}{a}\right); \qquad \tau_1 \equiv \left(0, \frac{a}{2}, \frac{a}{2}\right); \quad \text{etc.} ,$$

it is easy to see that $D(\boldsymbol{g}) = 4$ if $l$, $m$, $n$, have the same parity, $D(\boldsymbol{g}) = 0$ otherwise.

The factor $\frac{1}{4}$ arises because we sum over a simple cubic lattice which contains only $\frac{1}{4}$ of the points in the FCC lattice.

In a similar way we can evaluate $D(g)$ for a diamond lattice, which consists of two FCC lattices one of which is obtained by the other by translation through a vector $\boldsymbol{\tau}_4 = (a/4, a/4, a/4)$. The result is

$$D(\boldsymbol{g}) = \tfrac{1}{8}\big(1 + \exp[i(\boldsymbol{g}\cdot\boldsymbol{\tau}_1)] + \exp[i(\boldsymbol{g}\cdot\boldsymbol{\tau}_2)] + \exp[i(\boldsymbol{g}\cdot\boldsymbol{\tau}_3)]\big)^2 \big|1 + \exp[i(\boldsymbol{g}\cdot\boldsymbol{\tau}_4)]\big|^2 . \tag{A.16}$$

## RIASSUNTO

Vengono studiati gli effetti di coerenza nella sezione d'urto totale per produzione di coppie in cristalli. Tali effetti dipendono dalla polarizzazione del fotone e possono essere usati per produrre ed analizzare fasci di raggi $\gamma$ linearmente polarizzati.